

# Design of a Microcontroller Based Automated Ice-cube Making Machine

I. F. Titiladunayo, R. A. Shittu

**Abstract**— Beyond homes and offices, the importance of ice in food service outlets, bars, hotels and some health care services industries, is very significant to quality service delivery as a lot of ice is needed within a short time and continuously for chilling and various other cooling purposes. However, the bulkiness and expensiveness of the manually operated locally made ice machines, which requires the need for a standby operator to carry out ice production activities should be eliminated through automation, in modern ice making machine designs. It is therefore an object of this paper to present the design of a portable self-contained automated ice-cube making machine suitable for small scale ice production within a short period of time, incorporating a control means which limits human interaction with the machine to starting the machine, and collecting ice cubes from the storage bin. The machine was designed, using the principle of vapour compression refrigeration system for the production of 24 cubes of ice measuring  $22 \times 22 \times 22$  mm at  $-15^{\circ}\text{C}$  from  $7.667 \times 10^{-4}$  m<sup>3</sup> of water within 30 minutes. The machine components and design results include: A R-134a reciprocating type compressor of 0.086kW capacity; a bare tube evaporator designed for 0.2984 kW refrigeration load; a finned-tube type condenser with 0.3847 kW capacity; and a water circulation pump of  $0.279 \times 10^{-3}$  kW pump power. The process of feeding water into the machine and harvesting of ice cubes is automated through the application of an electronic control system incorporating a PIC16F877A microcontroller. The control unit was designed and simulated on Proteus Design Suite while the programming codes was written in C language on MPLAB IDE.

**Index Terms**— Automation, design, ice-cube, hot-gas defrost, microcontroller, pic16F877A, refrigeration.

## I. INTRODUCTION

Refrigeration finds large scale industrial and domestic application in the production of ice. Ice making machines are manufactured in different sizes and capacities for the production of ice in various sizes and shapes ranging from ice-cube, to nugget and flake-type ice [1]. They are installed in food service outlets, hospitals, industries, bars, restaurants, hotels, laboratories, sport arenas and various other places where large quantities of ice are needed on a continuous basis. Among the prevalent use of ice, is in chilling of beverages at homes, offices, conferences, cocktail parties etc. In developing tropical countries like Nigeria, the demand for ice for chilling of drinks is high during the dry season [2], [4]. In efforts to ensure availability of ice and chilled beverages, Oladunjoye and Omogbemile [3] designed and constructed a two-compartment freezing unit; Mohammed *et al.* [4] developed a refrigerated cooling table to provide chilled

drinks at conferences and meetings; Nasir *et al.* [2] designed and carried out the performance evaluation of an ice block making machine.

In some areas of application of ice, it is required that ice is supplied continuously over time. In some cases, it is required that ice is readily available when needed such as when serving a cocktail. These necessitate the availability of an ice making machine that produces ice continuously, store the produced ice, and make it available on demand. Locally made ice making machines are bulky, expensive and usually requires a manual operator to fill ice trays, bags or molds with water, place them in the freezing chamber, and retrieve the formed ice when needed. The frozen ice often gets stuck in the molds or on the freezing surface which makes its retrieval a very difficult and tiring task. However, manual operation and the need for a standby operator could be eliminated through automation, in modern ice making machine designs.

There are extensive data and design models for the design of vapour compression refrigeration system components including evaporator, condenser, compressor, capillary tube and refrigerants which some can be found in [2], [4], [5], [6], and [20]. Pandey and Agrwal [7] also presents an extensive review of literature in the work titled, performance analysis of ice plant using ecofriendly refrigerant. Proper electrical control systems for refrigeration equipment components are essential to improve efficiency, performance and reliability. The use of microcontrollers for equipment control is increasing due to its simplicity and benefits. Harjono *et al.* [8] designed an automation control condensing unit to improve ice cube products using microcontroller. A control system was developed using Arduino Servarino Board to regulate the working of a cooling water pump, condenser fan motor, unscrew the valve of the refrigerant pressure and the running of compressor motor in a sequence to maintain brine temperature in range of  $-6^{\circ}\text{C}$  to  $-15^{\circ}\text{C}$ . Thein *et al.* [9] designed and developed a microcontroller-based air conditioning system. The air conditioner control card developed based on PIC16F877A was constructed on air conditioning system to control temperature values for heating and cooling process, and speeds for compressor motor and fan.

This paper centres on the design of a machine that could produce ice-cubes from feedwater on a continuous basis and with limited human interaction. The quantity of water fed into the machine, freezing temperature, residence time for ice in the machine molds, detachment of ice from the molds after formation and the ejection of ice-cubes from the molds to harvest bin are achieved automatically through the control unit of the machine.

I. F. Titiladunayo, Department of Mechanical Engineering, Federal University of Technology Akure, Akure, Nigeria, +2348037447426

R. A. Shittu, Department of Mechanical Engineering, Federal University of Technology Akure, Akure, Nigeria, +2348079767624

## II. METHODOLOGY

### A. Design Concept, Description and Operation of the Automated Ice-cube Making Machine

The machine consists of: a water supply system including a pump which automatically and continuously circulates water over a freezing surface (a mold) which is in thermal contact with the evaporator plate assembly; a refrigeration system having a compressor, a condenser, an expansion valve and an evaporator; and a hot gas defrost system which bypasses the high-pressure and high-temperature vaporized refrigerant compressor discharge from the condenser, which is fed to the evaporator, achieved by the opening of the hot gas valve so as to achieve ice releasing from the mold. It works based on the principle of vapour compression refrigeration system as shown by the schematic diagram presented in Fig. 1 showing the various components of the refrigeration system and refrigerant flow direction.

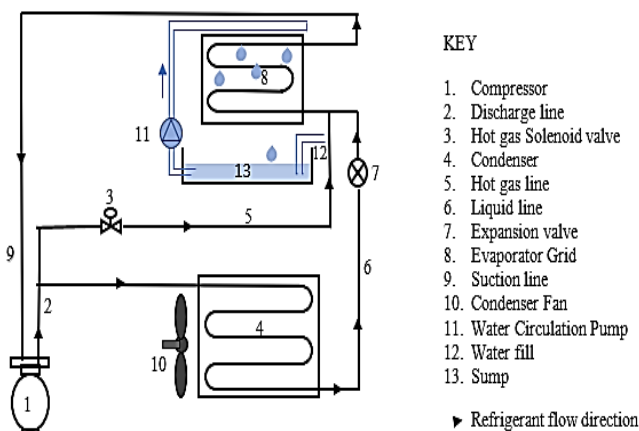


Fig. 1. Schematic diagram of the ice-cube making machine showing components and refrigerant flow

The machine is designed to work in two distinct modes: Ice-making and Harvest mode. The Ice-making mode occurs when water is circulated over the mold or freezing surface which is in contact with the surface of the evaporator and ice is being formed. The Harvest mode occurs when the bond between the ice and freezing surface is broken and the ice is released from the surface into the bin. In the Ice-making mode, the refrigeration system operates in a normal manner such that expanding refrigerant in the evaporator removes heat from the water flowing over the ice mold, freezing the water to form ice. A temperature sensor monitors the temperature of the suction line. Once a preset temperature is reached, the machine is switched to Harvest mode. During the Harvest mode, the hot gas solenoid valve opens which sends hot refrigerant from the compressor directly to the evaporator mounted on the back of the cube forming mold. The ice mold is heated by the hot refrigerant gas until the bond between the formed ice and the mold is broken and released. Once the formed ice is released from the mold, the Ice-making mode is activated, and thus, the cycle begins again. An electronic control system based on PIC microcontroller is incorporated to control the operations of the machine. The assembly (showing some internal components), orthographic and isometric views of the designed machine is shown in Fig. 2 and 3 respectively.

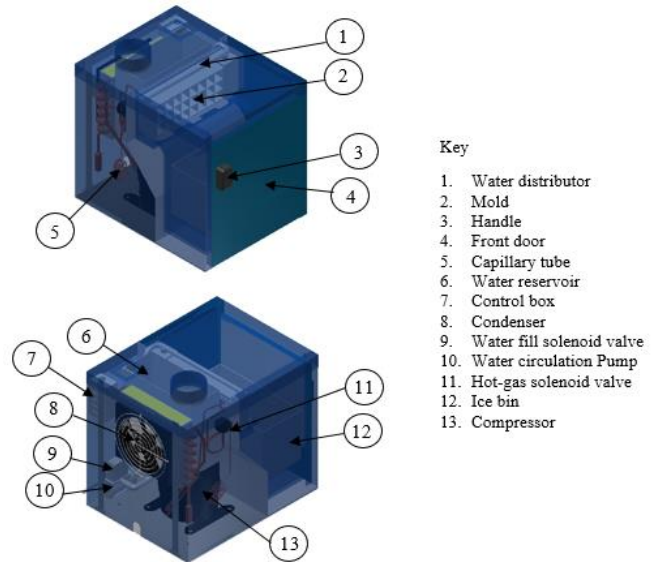


Fig. 2. Assembly of the Automated Ice-cube Making Machine

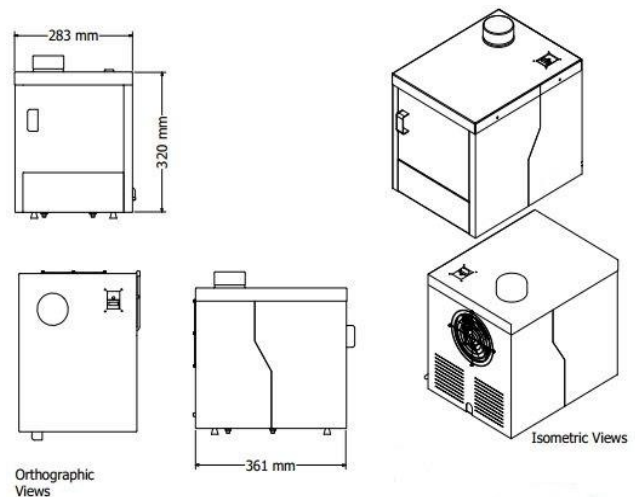


Fig. 3. Orthographic and Isometric Views of the Automated Ice-cube Making Machine

### B. General Design Considerations

The following basic requirements were considered in the design of the ice-cube making machine:

- 1) The machine is designed to produce 24 ice cubes of size  $22 \times 22 \times 22$  mm per production cycle;
- 2) For hard ice which will take longer time to defrost to be produced, the evaporator is designed to be maintained at  $-15^\circ\text{C}$ ;
- 3) The design ambient temperature is taken to be  $30^\circ\text{C}$  which is high enough to allow for extreme condition; and a design condensing temperature of  $40^\circ\text{C}$  is chosen to allow continuous condensation heat transfer to the environment;
- 4) The desired production time is 30 minutes so that ice cube is produced within a short period of time, and;
- 5) Portable design, as it is targeted for small scale ice production.

### C. Design of the Feedwater Supply System

When the ice-making machine starts, the water-fill solenoid valve opens allowing water to flow by gravity from

the water reservoir into the sump (see Fig. 4). When the sump is filled to the desired level, monitored by the water level sensor, the water- fill solenoid valve is then closed and the water circulation pump is activated. The water circulating pump transfers water from the sump upward through the water distribution channel, where it is distributed over the mold, through water jets located on the channel. Excess circulating water runs off the front edge of the mold and fall back into the sump, where it is recirculated over the mold as the freezing process takes place. Ice gradually builds on the mold as the process progresses in cycles. The water recirculation continues until the end of the ice-making cycle.

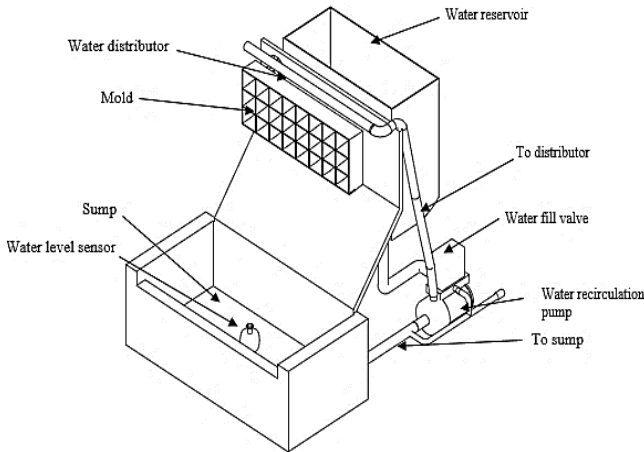


Fig. 4. Water Supply System

#### D. Design of the Feedwater Supply System

Water pump is required to transfer water through a total head of 410 mm in an 8.3 mm pipe. The capacity of the water circulation pump is determined for the design flowrate of 0.25 m<sup>3</sup> using (1) [10].

$$p_{pump} = \frac{Q\rho gH}{3.6 \times 10^6} \quad (1)$$

where:  $p_{pump}$  is the pump power in kW; Q is the flowrate in m<sup>3</sup>/h; H is the total head;  $\rho$  is the density of water, 1000 kg/m<sup>3</sup>; and g is acceleration of gravity, 9.8 m/s<sup>2</sup>.

#### E. Mold Design

The size and the geometry of the mold (as shown in Fig. 5) is based on the size and the number of ice cubes that is to be produced by the machine. It is made of stainless steel because of its high thermal conductivity and resistance to corrosion. It is tightly fused to the evaporator coil surface to facilitate heat transfer.

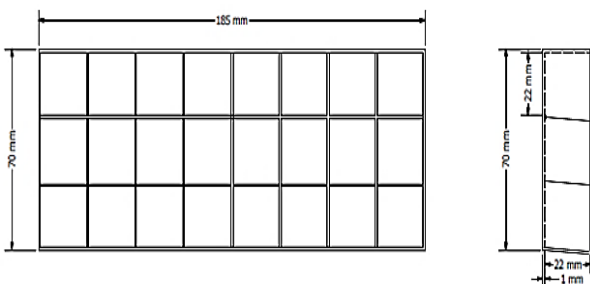


Fig. 5. Mold Design

The base where the ice sits is made inclined to allow the ice slide into the storage bin when released.

#### F. Determination of the Volume of Water for Circulation During Ice Production

Water is recirculated from the sump to form the ice. The amount of water in circulation is designed to be thrice the amount to needed to form the ice in a production cycle and was determined from (2). This is to allow enough water to be in the sump for recirculation by the pump throughout the ice-making cycle as well minimizing refrigeration load on the system.

$$V_{w_c} = (LBH) \times 24 \times 3 \quad (2)$$

where LBH are the length, breadth and height of the ice-cube respectively.

#### G. Refrigeration Load Determination

The sources of refrigeration load considered in this design are the product load and the wall gain load. Other sources of refrigeration load are not considered in this design as they do not constitute a significant part of the refrigeration load and/or are completely irrelevant. 10% of the total refrigeration load was added to the total load as a factor of safety as suggested in [5].

**Product load ( $\dot{Q}_{product}$ ):** Heat removed from the water itself as it is cooled to the desired temperature constitute the product load. To freeze the water from its initial temperature ( $T_i$ ) to ice at the desired final temperature ( $T_f$ ) the total product load is given by the summation of the heat removed from the water when cooling to the freezing point, the latent heat removed while freezing, and the heat removed as it is further cooled to the desired subfreezing temperature which is given by (3).

This is expressed as:

$$\dot{Q}_{product} = \frac{m_w [C_{p,w}(T_i - T_o) + h_{latent} + C_{p,ice}(T_o - T_f)]}{\Delta t_p} \quad (3)$$

where:  $C_{p,w}$  is the specific heat of water (kJ/kgK);  $C_{p,ice}$  is the specific heat of ice (kJ/kgK);  $h_{latent}$  is the latent heat of fusion (kJ/kg);  $t_p$  is the desired production time in secs and;  $T_o$  is the freezing temperature of water.

**Heat gain through the wall ( $\dot{Q}_{wall}$ ):** The heat gain through the wall of the ice machine is determined using (4) [5].

$$\dot{Q}_{wall} = A_s U \Delta T \quad (4)$$

where:  $A_s$  is the calculated outside surface area of the walls (m<sup>2</sup>); U is the overall heat transfer coefficient (W/m<sup>2</sup>K) and;  $\Delta T$  is the temperature differential across the wall.

The wall of the machine consists of the outer layer made of aluminium, insulation layer made of polystyrene and the inside layer made of aluminium. Thus, the overall heat transfer coefficient (U) is expressed as:

$$U = \frac{1}{\frac{1}{h_o} + \frac{x_{al}}{k_{al}} + \frac{x_p}{k_p} + \frac{x_{al}}{k_{al}} + \frac{1}{h_i}} \quad (5)$$

where:  $h_o$  and  $h_i$  are convective heat transfer coefficient at the outer and inner surface respectively;  $x_{al}$  is thickness of aluminium sheet;  $x_p$  is the thickness of the polystyrene insulation;  $k_{al}$  and  $k_p$  are the thermal conductivity of aluminium and polystyrene respectively.

H. Determination of the VCRC State Point Parameters and Performance

The various state point parameters were obtained using a simple vapour compression refrigeration cycle (VCRC) on pressure-enthalpy chart for R-134a. The cycle diagram represented on a p-h chart is as shown in Fig. 6.

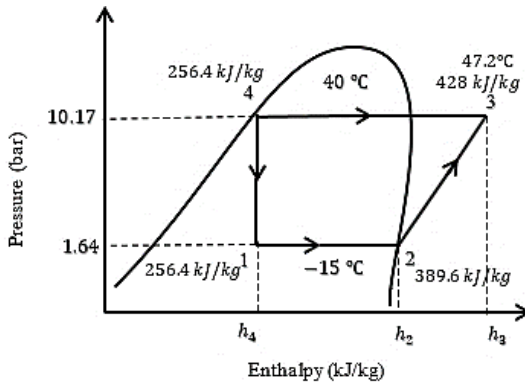


Fig. 6. Representation of State Point on Pressure-Enthalpy Chart

The refrigeration effect (R.E), refrigerant mass flow rate and Coefficient of performance (COP) were determined using (6), (7), and (8) respectively [5].

$$R.E = h_2 - h_1 \tag{6}$$

$$\dot{m}_r = \frac{\text{Total Refrigeration Load } (Q_{total})}{h_2 - h_1} \tag{7}$$

$$COP = \frac{h_2 - h_1}{h_3 - h_2} \tag{8}$$

I. Compressor Design

The capacity of the compressor required with its swept volume is determined with (9), and (10) respectively [11].

$$P_{comp} = \dot{m}_r (h_3 - h_2) \tag{9}$$

$$V_{sv} = \dot{m}_r \times v_i \tag{10}$$

where:  $P_{comp}$  is compressor capacity (kW);  $h_3$  is enthalpy of superheated refrigerant vapour discharged from the compressor;  $h_2$  is enthalpy of saturated refrigerant vapour at the suction line; and  $v_i$  is the specific volume of refrigerant vapour at the inlet of the compressor.

J. Evaporator Assembly Design

The evaporator assembly consists of the mold and the evaporator tubing (as shown in Fig. 7), welded together in order to provide good thermal contact between them. The evaporator tubing is made of copper because of its high thermal conductivity and its ease of fabrication compared to some other materials.

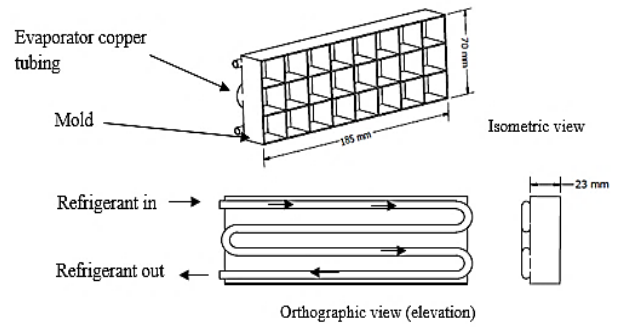


Fig. 7. Evaporator Assembly

The length of the evaporator tube needed to convey the refrigerant into the cooling space to effect the required heat transfer (heat absorption) is determined thus. A copper tube of 4.76 mm (3/16 inches) external diameter and 3.26 mm (0.128 inches) internal diameter was selected for the evaporator tubing from available standard sizes [19]. The heat transferred through the wall of the tube to the vaporizing refrigerant is expressed as [5].

$$\dot{Q} = A_s U T \tag{11}$$

where:  $\dot{Q}$  is the heat transferred through the surface of the evaporator tube (W);  $A_s$  the outside surface area of the evaporator tube ( $m^2$ );  $U$  is the overall heat transfer coefficient ( $W/m^2K$ );  $T$  is the temperature difference between the flowing water and the refrigerant inside the tube

The surface area of the evaporator tube is given by

$$A_s = 2\pi r_o L \tag{12}$$

The overall heat transfer coefficient is expressed in (13) is derived by stepwise analysis of the heat transfer by convection on the outside, conduction through the surface of the tube and convection on the inside of the tube. The temperature difference from each of the equations is made the subject of relation and then added together to give an expression which is compared to (11) to factor out the expression for  $U$ .

$$U = \frac{1}{\frac{r_o}{h_i r_i} + \frac{r_o}{k_{co}} \ln\left(\frac{r_o}{r_i}\right) + \frac{1}{h_o}} \tag{13}$$

The inside heat transfer coefficient is expressed as [12]

$$h_i = \frac{Nu \times k_r}{2r_i} \tag{14}$$

where  $k_r$  is the thermal conductivity of the refrigerant at the evaporating temperature.

Nusselt Number ( $Nu$ ) as defined by Dittus-Boelter is expressed as

$$Nu = 0.023(Re)^{0.8} (Pr)^{0.4} \tag{15}$$

Reynolds Number ( $Re$ ) is expressed as [11]

$$Re = \frac{\rho V D_i}{\mu_r} \tag{16}$$

$$V = \frac{\dot{m}_r}{\rho A_i} \quad (17)$$

and Prandtl Number,  $Pr$ , is expressed as [11]

$$Pr = \frac{C_{p,r} \mu_r}{k_r} \quad (18)$$

where:  $\mu_r$  is the viscosity of the refrigerant;  $C_{p,r}$  is the specific heat capacity at constant pressure of the refrigerant;  $V$  is the mean velocity of flow.

Thus, the length of the tube required for the heat transfer is expressed as

$$L = \frac{\dot{Q}}{\pi D_o U \Delta T} \quad (19)$$

### K. Condenser Design

A finned-tube type condenser is designed as the condensing unit of the ice-making machine. It consists of: the condenser tubing; plate-fins which facilitates heat transfer; and a fan which blows air over the fin-tube assembly. The condenser fins are made of aluminium and the tubing is made of copper because of its high thermal conductivity. A model of the condenser is shown in Fig. 8. The tube diameter, 6.35 mm (1/4 inches) and 4.83 mm (0.190 inches) outside and inside diameter respectively, is selected from available standard sizes in the market. Heat transfer analysis (refrigerant side and air side) and determination of condenser tube length required is done in great detail. The flow of refrigerant in the condenser is both in single-phase and two-phase as refrigerant enters the condenser as superheated vapour and leaves as saturated liquid. Thus, the calculations are done separately for single and two-phase respectively.

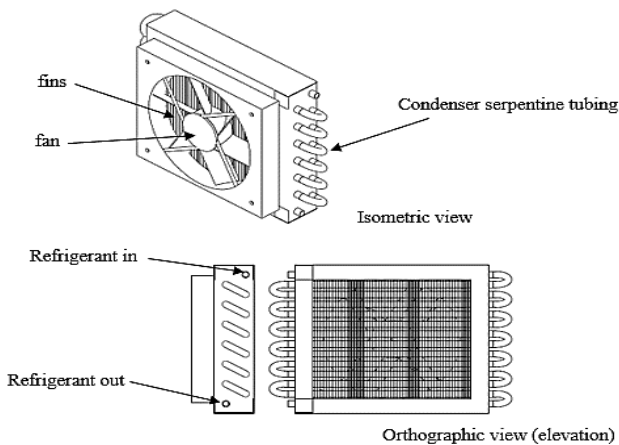


Fig. 8. Condenser Design Model

The amount of heat rejected to the surrounding through the condenser during the condensation process is obtained using (20).

$$\dot{Q}_{cond} = \dot{m}_r (h_3 - h_4) \quad (20)$$

where  $h_3$  and  $h_4$  are the enthalpies of the refrigerant entering and leaving the condenser.

(i) Refrigerant-side heat transfer and pressure drop calculations

The area through which the refrigerant flow inside the condenser tube is given by (21).

$$A_i = \frac{\pi D_i^2}{4} \quad (21)$$

The refrigerant mass flux ( $G$ ) is determined using (22) [13].

$$G = \frac{\dot{m}_r}{A_i} \quad (22)$$

Single-phase flow (refrigerant-side)

On the refrigerant side, single-phase (vapour) flow occurs in the superheated region at the entry of the condenser. The Reynold number ( $Re_{sp}$ ) is defined as [13]

$$Re_{sp} = \frac{GD_i}{\mu_{sp}} \quad (23)$$

The properties of R134a refrigerant are taken at the entry temperature 47.2°C.

The flow being turbulent, Nusselt number is defined as [21]

$$Nu_u = \left( \frac{f}{8} \right) (Re_{sp} - 1000) \frac{Pr}{1 + 12.7 \sqrt{\frac{f}{8}} (Pr^{2/3} - 1)} \quad (24)$$

where  $f$  is Friction factor. For  $2300 < Re < 5 \times 10^6$  friction factor is [2]

$$f = \frac{1}{(1.82 \log Re_{sp} - 1.64)^2} \quad (25)$$

The single phase (vapour) heat transfer coefficient ( $h_{sp}$ ) is thus determined using (26) [12].

$$h_{sp} = \frac{Nu_{sp} k_{sp}}{D_i} \quad (26)$$

The pressure drop ( $\Delta P$ ) across the tube in the single-phase region is determined by applying the standard pipe pressure drop equation for straight section of the tube given by (27) [12].

$$\Delta P = \frac{f G^2 L}{\rho_{sp}} \quad (27)$$

where:  $\mu$  is the viscosity of the refrigerant; subscript  $sp$  is single-phase; and  $\rho$  is the density of refrigerant

Two-phase flow (refrigerant-side)

The Reynold number of the liquid phase and vapour phase in the two-phase region is given by (28) and (29) respectively [13].

$$Re_l = \frac{G(1-x)D_i}{\mu_l \left( 1 + \sqrt{a_{vf}} \right)} \quad (28)$$

$$Re_v = \frac{GxD_i}{\mu_v \left( \sqrt{a_{vf}} \right)} \quad (29)$$

where: subscript *l* and *v* is represent liquid and vapour phase respectively; *x* is the vapour fraction; and *a<sub>vf</sub>* is the void fraction given by (30) [14].

$$a_{vf} = \left[ 1 + \left( \frac{\rho_v}{\rho_l} \right)^{0.65} \left( \frac{\mu_l}{\mu_v} \right)^{0.13} \left( \frac{1-x}{x} \right)^{0.74} \right]^{-1} \quad (30)$$

The properties of R134a refrigerant are obtained at the condensing temperature 40°C.

The sum of the frictional and momentum pressure drops for the two-phase region is determined using (31) [13].

$$\Delta P = \frac{f_i G^2 x^2 L}{2 \rho_v a_{vf}^{2.3} D_i} \quad (31)$$

where: *P* is the sum of frictional and momentum pressure drop; *f<sub>i</sub>* is the interfacial friction factor; *L* is the length.

The interfacial friction factor is given as [13]

$$f_i = BX^a Re_l^b \beta^c f_l \quad (32)$$

where *B*, *a*, *b*, *c* are constants whose value depends on the value of the Reynold's number.

*X* is the Martinelli parameter obtained using (33)

$$X = \left( \frac{\rho_v}{\rho_l} \right)^{0.5} \left( \frac{\rho_l}{\rho_v} \right)^{0.1} \left( \frac{1-x}{x} \right)^{0.9} \quad (33)$$

and the *β* is the surface tension parameter given as [14]

$$\beta = \frac{j_l \mu_l}{\sigma} \quad (34)$$

where *σ* is the surface tension and *j<sub>l</sub>* is the liquid superficial velocity.

The local heat transfer coefficient in the two-phase region of the refrigerant side is obtained using (35) given in [15].

$$h_{tp} = \frac{\rho_l c_{p,l} (\tau_i / \rho_l)^{0.5}}{T^+} \quad (35)$$

where *c<sub>p,l</sub>* is specific heat capacity at constant pressure of the refrigerant liquid, *T<sup>+</sup>* is the turbulent dimensionless temperature and *τ<sub>i</sub>* is the liquid interfacial shear stress.

(ii) Air-side pressure drop and heat transfer calculations

The minimum flow (*A<sub>min</sub>*) area for the air-side of the condenser and the air mass flux (*G<sub>max</sub>*) is given by (36) and (37) respectively [14].

$$A_{min} = (F_{sp} - F_{th}) X_{tr} \quad (36)$$

where: *F<sub>sp</sub>* is the fin spacing, *F<sub>sp</sub>* = 1/*F<sub>pi</sub>* = 1/*F<sub>pi</sub>*; *F<sub>pi</sub>* is the fin pitch; *F<sub>th</sub>* is the fin thickness; and *X<sub>tr</sub>* *X<sub>tr</sub>* is the transverse or vertical spacing of the tubes

$$G_{max} = \frac{\dot{m}a}{A_{min}} \quad (37)$$

The air-side convective heat transfer coefficient is defined as

$$h_a = j_{colb} c_{p,a} U_a \rho_a Pr_a^{2/3} \quad (38)$$

where *j<sub>colb</sub>* is Colburn j-factor

The pressure drop of the air-side across the fin is obtained using (39) [16].

$$\Delta P_{fin} = f_{fin} v_{m,a} \frac{G_{max}^2 A_{fin}}{2 A_{min}} \quad (39)$$

where: *v<sub>m,a</sub>* is the mean specific volume of air; *A<sub>fin</sub>* is the fin surface area; and *f<sub>fin</sub>* is the fin friction factor expressed as [16]

$$f_{fin} = 1.7 Re_{lo}^{-0.5} \quad (40)$$

The overall heat transfer calculations

Neglecting fouling, wall thermal resistance and assuming the refrigerant side surface efficiency is one, the overall heat transfer coefficient (*UA*) is defined as [17]

$$UA = \left( \frac{1}{\eta_a \bar{h}_a A_a} + \frac{1}{\bar{h}_r A_r} \right)^{-1} \quad (41)$$

where: *η<sub>a</sub>* is the air-side surface efficiency; *h<sub>a</sub>* is the average air-side heat transfer coefficient; *h<sub>r</sub>* is the average refrigerant-side heat transfer coefficient; *A<sub>r</sub>* and *A<sub>a</sub>* is the respective refrigerant and air side heat transfer area.

The air-side surface efficiency is obtained using (42) [12]

$$\eta_a = 1 - \frac{A_{fin}}{A_a} (1 - \eta_{fin}) \quad (42)$$

where the fin efficiency (*η<sub>fin</sub>*) is defined as [17]

$$\eta_{fin} = \frac{\tanh(\lambda_{es} r \phi)}{\lambda_{es} r \phi} \quad (43)$$

where *λ<sub>es</sub>* is the standard extended surface parameter defined as [17]

$$\lambda_{es} = \left( \frac{2 \bar{h}_a}{k_{fin} F_{th}} \right)^{0.5} \quad (44)$$

where *k<sub>fin</sub>* is the thermal conductivity of the fin material; and [14]

$$r \phi = X_{lo} + \frac{X_{tr}}{2} \quad (45)$$

The total heat transfer rate is then determined using the general heat transfer equation given by (46). The result obtained here is compared with the designed heat rejected by the condenser calculated with (20) until the difference is less than 1%, if not, then an iterative procedure is followed.

$$\dot{Q}_{cond} = UA\Delta T_m \quad (46)$$

Where  $T_m$  is the logarithmic mean temperature difference expressed as [11]

$$\Delta T_m = \frac{(T_{ref,i} - T_{air,i}) - (T_{air,l} - T_{air,i})}{\ln \left[ \frac{(T_{ref,i} - T_{air,i})}{(T_{air,l} - T_{air,i})} \right]} \quad (47)$$

where:  $T_{ref,i}$  is temperature of the refrigerant at the inlet;  $T_{air,i}$  is the temperature of air entering; and  $T_{air,l}$  is the temperature of air leaving

#### Power requirement of the condenser fan

The power required for the condenser fan is expressed in terms of the pressure drop in the air-side across the condenser given by (48).

$$P_{fan} = \Delta P_a \frac{\dot{m}_a}{\rho_a} \quad (48)$$

where  $P_a$  is the pressure drop in the air-side and  $P_{fan}$  is the fan power requirement.

#### L. Capillary Tube Design

Since capillary tubes are available in specific sizes (diameter and length), a diameter of 0.991 mm is selected, and then the required length is determined for the desired pressure drop to be achieved. The tube is divided into 5 segments (1 and 2, 2 and 3, 3 and 4, 4 and 5, 5 and 6) as represented by the pressure-enthalpy diagram shown in Fig. 9. The pressure drop in each of the segments is determined and the corresponding length. The entry and the exit points of each of the segments is denoted by nodes (1, 2, 3, 4, 5 and 6). The overall length of the capillary tube is then obtained as the submission of length of all the segments. The process is assumed to be isenthalpic.

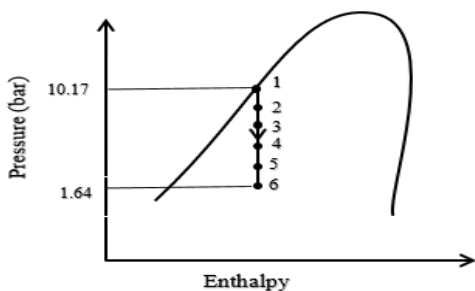


Fig. 9. Segmentation of Expansion Process on p-H Diagram

The area of flow of the refrigerant in the capillary tube and its mass flux is obtained using (49) and (50)

$$A_{capi} = \frac{\pi D^2}{4} \quad (49)$$

$$G = \frac{\dot{m}_r}{A_{capi}} \quad (50)$$

The length of the capillary tube for each of the segments is obtained using (51) with an assumption that the flow is one-dimensional, incompressible and single-phase [18].

$$\Delta L_i = \frac{-\Delta P - G\Delta V}{\left(\frac{G}{2D}\right)(fV)_{mean}} \quad (51)$$

where: subscript  $i$  represents the nodes (1 to 6);  $\Delta P$  is the pressure drop;  $\Delta V$  is the velocity differential;  $V$  is the velocity of refrigerant at each of the nodes; and  $f$  is the corresponding friction factor.

The properties of the refrigerant and friction factor are evaluated at each node. In order to achieve this, the dryness fraction ( $x$ ) for each node is first determined using (52) [11].

$$x_i = \frac{h_i - h_{f_i}}{h_{g_i} - h_{f_i}} \quad (52)$$

and then specific volume and viscosity are obtained using (53) and (54)

$$v_i = v_{f_i} + x_i(v_{g_i} - v_{f_i}) \quad (53)$$

$$\mu_i = \mu_{f_i} + x_i(\mu_{g_i} - \mu_{f_i}) \quad (54)$$

The friction factor and velocity of refrigerant at each node is determined using (55) and (56) respectively [12].

$$f_i = \frac{0.32}{Re_i^{0.25}} \quad (55)$$

$$V_i = Gv_i \quad (56)$$

$$Re_i = \frac{DG}{\mu_i} \quad (57)$$

where  $i = 1$  to 6

#### M. Automation of the Machine

The electrical control system is designed to achieve the following control operations in order to automate ice-cube production with the machine:

- 1) Opening the water solenoid valve for a predetermined time before the ice-making cycle begins, in a condition where the water pump and compressor are not active.
- 2) Allowing the water level sensor mounted within the sump to detect whether or not the level of water in the sump has reach the required level and repeating this at the beginning of every ice production cycle.
- 3) Starting the ice-making cycle when the level of water in the sump has reached the required level, by starting the compressor, water circulation pump and condenser fan in a condition where the hot gas defrost solenoid valve is closed.
- 4) Determining when to end the ice-making cycle and start the harvest cycle by opening the hot gas defrost valve in a condition where the water circulation pump is deactivated.
- 5) Determining when to end the harvest cycle and to carry out the initial water supply before starting the ice-making cycle.

The control system design showing input components, the controller and the output is illustrated in the block diagram shown in Fig. 10.

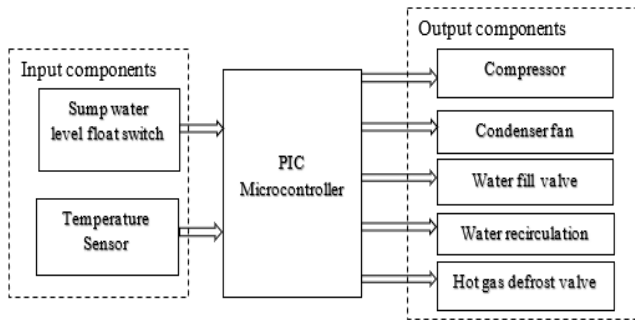


Fig. 10. Block Diagram of the Control System Showing Various Components of the System

N. System Operation Sequence and Control Instructions

Flowchart diagram of the program of instructions is shown in Fig. 11.

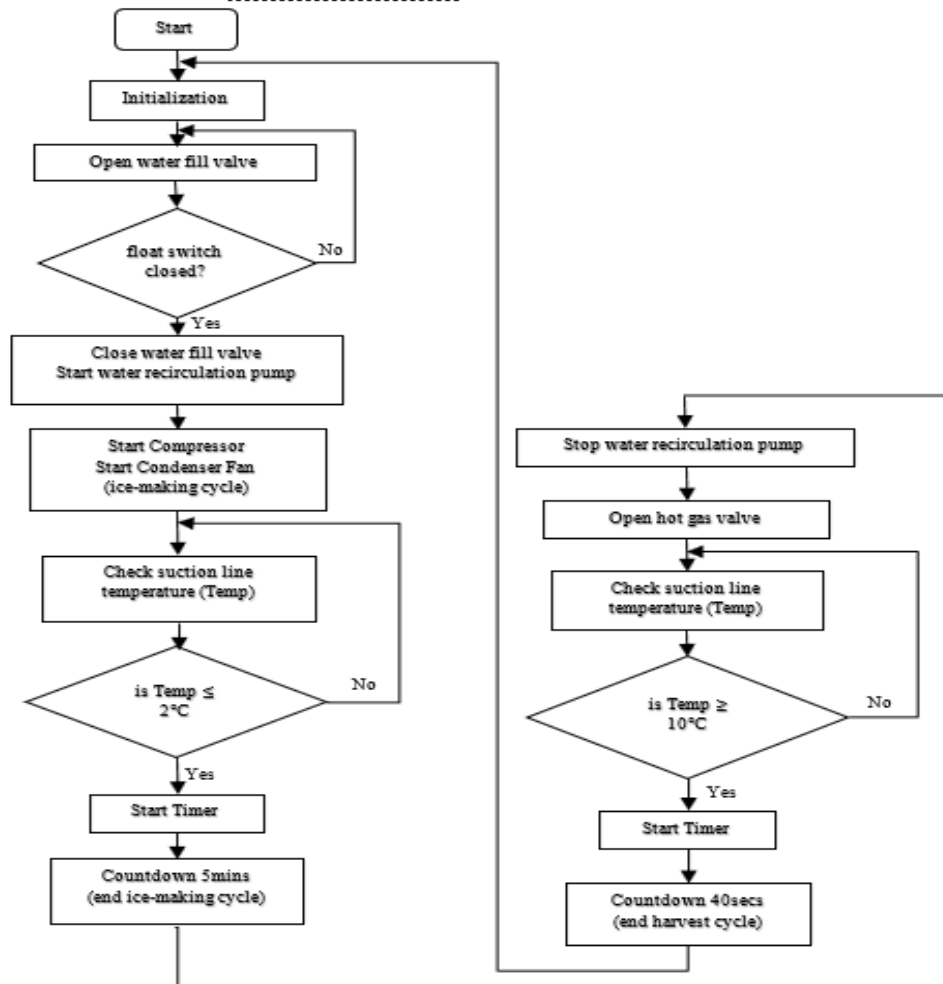


Fig. 11. Flow Diagram of the Program of Instruction

When the machine is powered on, the system starts with initializing procedure. Then an open water fill valve command is executed if the float switch is closed, in which the solenoid water fill valve is energized under the control of a relay switch. The water fill valve is maintained in open position which allows fresh water from the reservoir to flow into the sump. If the float switch is open, then the water fill valve is de-energized in which the fill valve is closed. Then the water circulation pump is energized under the control of a relay switch. The switching transistor then activates the electric motor of the compressor and the condenser fan controlled by relay switches. At this point the ice-making cycle begins. The temperature of the suction line is monitored through the temperature sensor installed on the suction line and stored in the RAM. The controller then continues to check whether or not the suction line temperature is below 2 °C. When it is below 2 °C, the microcontroller timer is started

to countdown 5 minutes. When the countdown is complete, the ice-making cycle ends.

The switching transistor then de-energize the water recirculation pump while the movable contact of a relay switch is switched over to energize the solenoid of hot gas valve. The hot gas valve opens and allow hot refrigerant gas to flow into the evaporator and this is the beginning of the harvest cycle. The temperature of the suction line is then monitored again and stored in the RAM. The controller then continues to check the temperature sensor input signal whether or not the suction line temperature is above 10°C. When it is above 10 °C, a timer is started which countdown 40 seconds. When the countdown is complete, the harvest cycle ends. The closed contact of the normally open relay switch is opened to de-energize the solenoid of the hot gas valve. The system then starts to initialize again to begin another cycle.

O. Control Circuit Schematic Design

Fig. 12 shows the control circuit design schematics. There are two inputs which are provided by the DS18B20 temperature sensor and the water level sensor. The temperature sensor is connected to the PIC16F877A through RA0 pin. The GND and VDD wires are connected to the ground and +5 V DC of the power supply. The float switch is connected at one of its ends to the ground and is connected to the controller through RA1 pin. +5 V from the power supply is supplied to power the PIC16F877A through the MCLR/Vpp pin. The ULN2003A is used to drive the desired output loads. The relay switch includes a relay coil which is grounded at one end and connected at its other end to the collector of a switching transistor. When the transistor is

turned on, the relay coil is energized to close the normally open contact. The electric motor of compressor is connected at its one end to the normally open contact of a relay switch and at its other end to the input. When supplied with the source voltage 230 V, the relay coil is energized to close the normally open contact. Pin RC1 and RC2 are used for the control of water recirculation pump and water fill valve respectively interposed by the ULN2003A which provides the 12 V required to power them. The condenser fan is operated by the controller through a solid-state relay connected at one of its ends to PIN RB0 of the microcontroller. The hot gas defrost solenoid valve and control button is connected on the circuit as shown in Fig. 12.

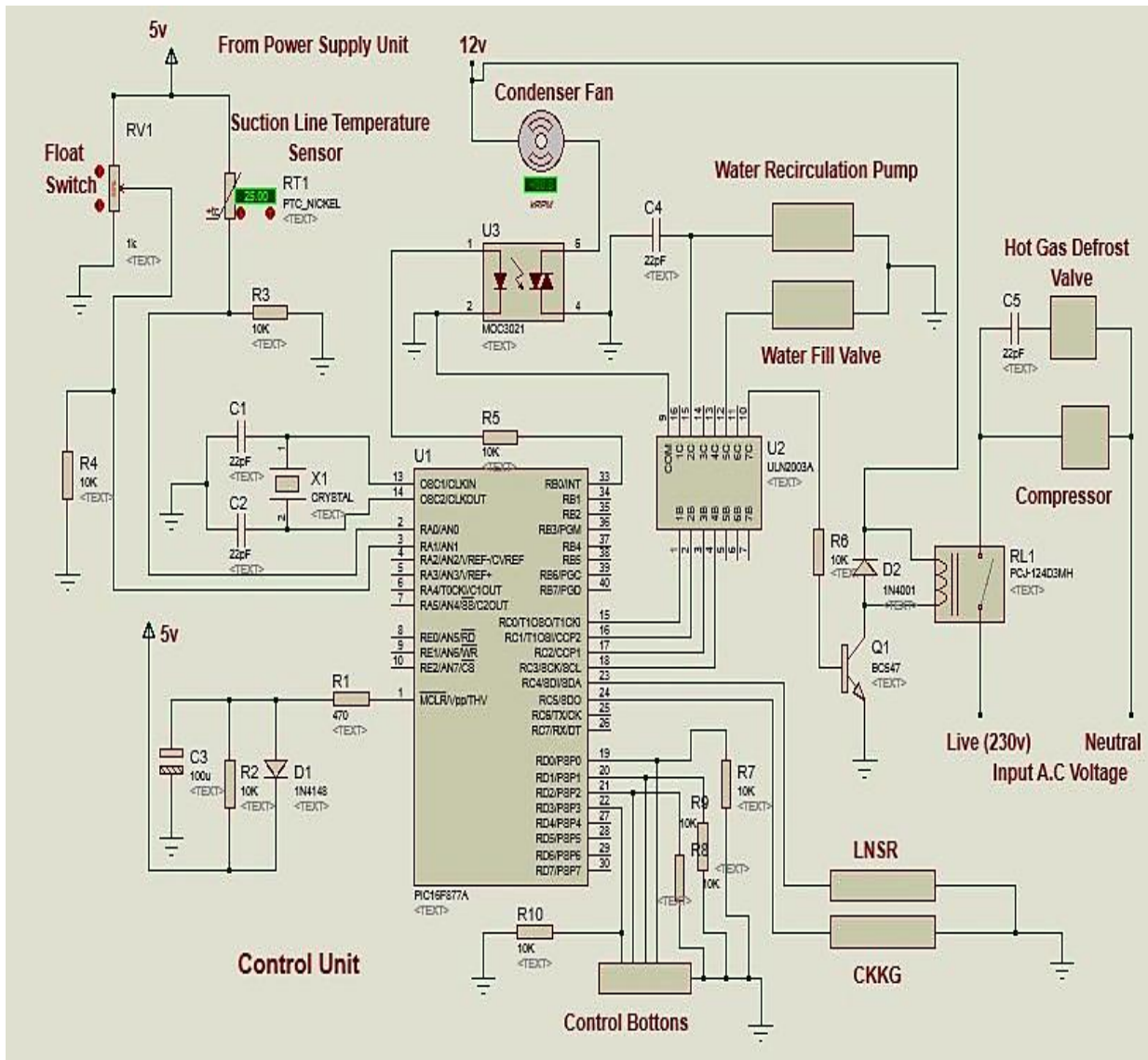


Fig. 12. Control Circuit Design Schematics

P. Power Supply Circuit Schematic Design

Fig. 13 shows the power supply circuit design schematics. The power supply unit is designed to produce 5 V DC, 12 V DC and 230 V AC for the control system components. 5 V DC is supplied to power the microcontroller, the temperature sensor and other components with 5 V DC power

requirement. 12 V DC is supplied to energize relays, condenser fan, the pump and other components requiring 12 V DC. 230 V AC is supplied to power AC components such as the compressor and hot gas valve. A voltage regulator, IC 7805 was used to produce a constant +5 V regulated voltage.

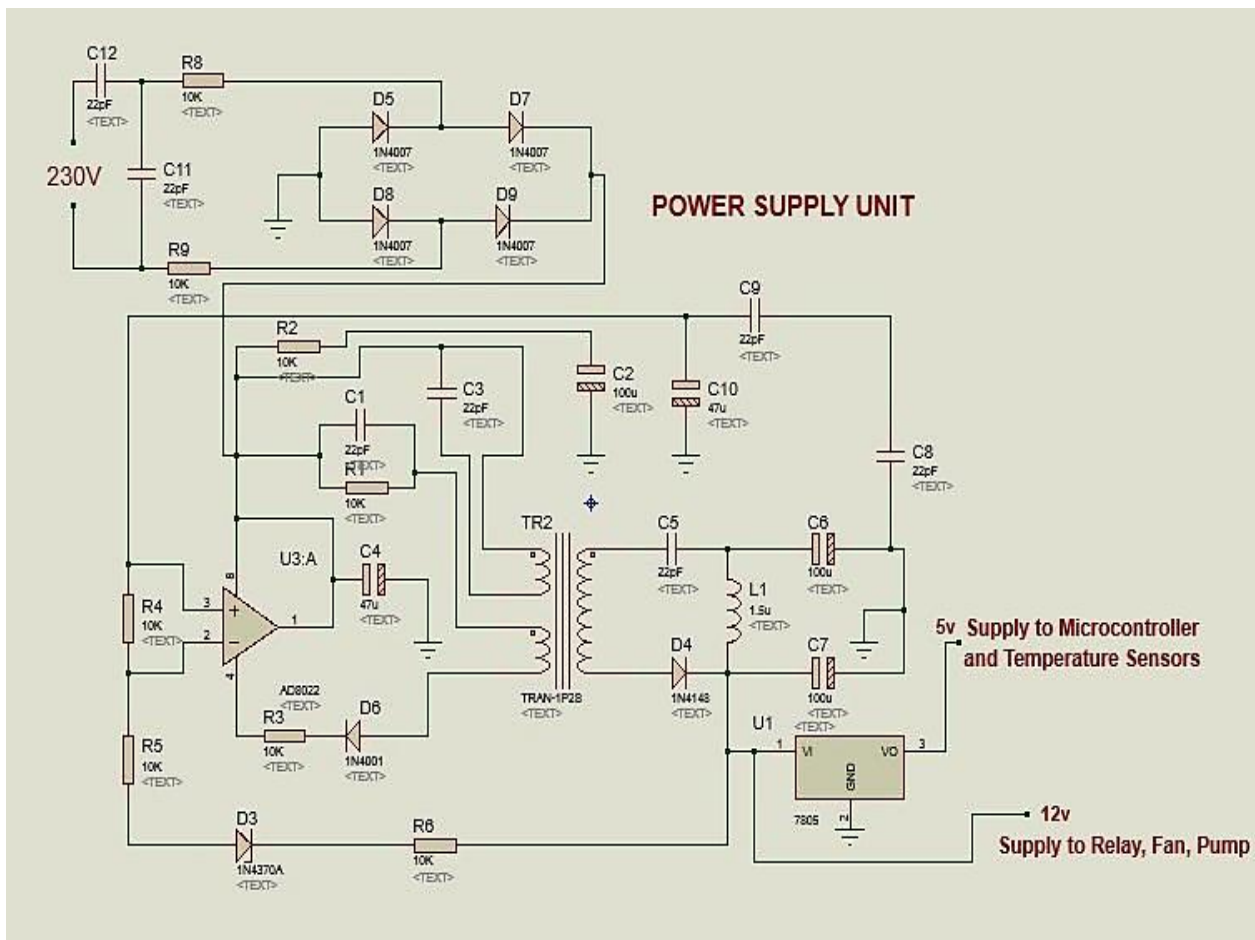


Fig. 13. Power Supply Circuit Design

III. RESULTS AND DISCUSSIONS

The results from the system components theoretical design are presented in Tables 1 to 5. The essence of the evaporator design is to determine the heat transfer area, the overall heat transfer coefficient and the required length of the evaporator tube, based on the design conditions for the necessary heat transfer to be achieved.

Table 1: Evaporator Design Results

Parameters	Value/Unit
Evaporating temperature	-15 °C
Evaporating pressure	1.64 bar
Refrigerant mass flow rate	0.00224 kg/s
Total refrigeration load	0.298397 kW
Refrigeration effect	133.2 kJ/kg
Evaporator tube length	5.35 m
Tube diameter (internal/external)	3.26 mm/4.76 mm
Overall heat transfer coefficient	82.83 W/m <sup>2</sup> K
Mean velocity of fluid flow	0.1998 m/s

Table 2: Compressor Design Results

Parameters	Value/Unit
Compressor capacity	0.086 kW
Swept volume	2.703 × 10 <sup>-4</sup> m <sup>3</sup> /s
Compressor clearance volume	0.208 × 10 <sup>-6</sup> m <sup>3</sup>

Results of the condenser design is presented in Table 3. The condenser design was done quite extensively with great deal of attention paid to geometric details such as the length of the serpentine tube, fin configuration, and the overall size of the condenser due to space requirement.

The flow of the refrigerant in the condenser tube is both in single-phase and two-phase. The pressure drop at the refrigerant side in the single-phase region is 4.225 Pa, while in the two-phase region, it is higher with 935.095 Pa as the pressure drop in the two-phase region is due to friction and acceleration. Also, heat transfer is lower in the single-phase region than in the two-phase region due to the lower heat transfer coefficient of 349 W/m<sup>2</sup>k in the single-phase region compared to 2112.89 W/m<sup>2</sup>k in the two-phase region. The

air side pressure drop and heat transfer coefficient are 36.7 Pa and 152.54 W/m<sup>2</sup>k respectively. Forced convection is preferred on the air side as the air side heat transfer coefficient is much lesser than that of the refrigerant side, thus, having dominant effect on the overall heat transfer.

Table 3: Condenser Design Results

Parameters	Value/Unit
Ambient temperature	30 °C
Condensation Temperature	40 °C
Tube diameter (internal/external)	4.83 mm/6.35 mm
Pressure drop	971.795 Pa
Condenser capacity	384.7 W
Total length of the condenser tube	2 m
Overall heat transfer coefficient	98.9 W/m <sup>2</sup> K
Fin thickness	0.15 mm
Fin efficiency	42.36%
Fan power	0.0255 W

The capillary tube plays an important role in dropping the pressure of the refrigerant in the system from the condensation pressure to the evaporating pressure. Since the temperature, pressure and vapor fraction vary along the length of the capillary tube, the calculation had to be done by dividing the length into finite segments. The designed capillary tube length and diameter can be seen in Table 4. The variation of refrigerant pressure and temperature with length of the tube is presented in Fig. 14.

Table 4: Capillary Tube Design Results

Parameters	Value/Unit
Diameter of the tube	0.991 mm
Length	1.9141 m

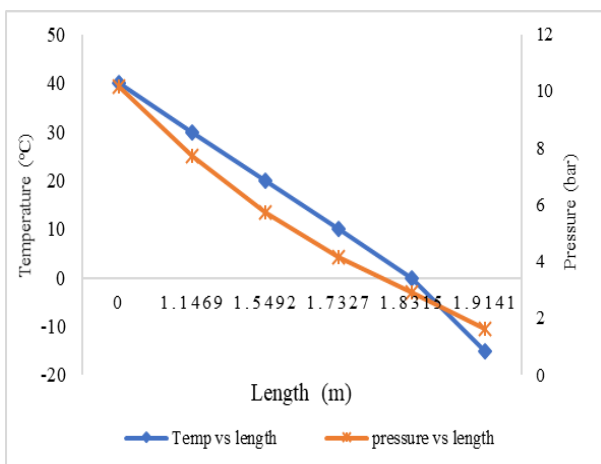


Fig 14. Temperature and Pressure Variation with Length of Capillary Tube

Table 5: Water Circulation Pump Design Results

Parameters	Value/Unit
Pump power	0.279 W
Flowrate	0.25 m <sup>3</sup> /h
Discharge orifice diameter	8.2 mm
Head	2.1 m

#### IV. CONCLUSION

The development of an automated machine for the production of ice-cubes is a need driven project. The purpose of this paper is to present the design of a machine which can be used for the continuous production of ice-cubes within a short period of time while human involvement with the machine is eliminated through automation. A portable self-contained ice-cube making machine suited for small scale ice production was designed. The process of feeding water into the mold for freezing, harvesting of the formed ice and the operation of the machine is automated by an electronic control system comprising of a temperature sensor, water level sensor, solenoid valves, and other electronic components including resistors, capacitors, transistors, relays, diode controlled by PIC16F877A microcontroller.

#### REFERENCES

- [1] K. Angelo, and F. Don, *A Field Study to Characterize Water and Energy Use of Commercial Ice Machines and Quantify Saving Potential*. San Ramon, CA: Fisher-Nikel Inc, 2007.
- [2] A. Nasir, A. Mohammed, A. S. Adegoke, and H. T. Abdulkarim, "Design and performance evaluation of an ice block making machine," *ARPJ Journal of Science and Technology*, 2013, 3(4), 332-339.
- [3] A. O. Oladunjoye, and D. Omogbemile, "Design and construction of two compartment freezing unit," 2003, pp. 10-14.
- [4] A. Mohammed, A. E. Elaigu, A. A. Adeniyi, and A. B. Hassan, "Development and evaluation of a prototype refrigerated cooling table for conference services," *International Journal of Engineering and Technology (IJET)*, 2012, 4(2), 97-108.
- [5] R. J. Dossat, and T. J. Horan, *Principle of Refrigeration*. 5th Edition, New Jersey: Prentice Hall, 2002.
- [6] B. O. Bolaji, M. A. Akintunde, and T. O. Falana, "Comparative analysis of performance of three ozone-friendly HFC refrigerant in a vapour compression refrigerator," *Journal of Sustainable Energy and Environment*, 2011, 2(2), 61-64.
- [7] P. Pandey, and A. B. Agrwal, Performance analysis of ice plant using ecofriendly refrigerant. *International Journal of Advanced Technology & Engineering Research (IJATER)*, 2015, 5(1), 42-50.
- [8] P. S. Harjono, A. A. Kristi, B. Susanto, A. Risdiyanto, and K. Ismail, "Design of Automation Control Condensing Unit to Improve Ice Cube Products Using Microcontroller," *Asian Transactions on Engineering*, 2015, 5(4), 1-6.
- [9] T. S. Thein, S. L. Kyaw, M. N. Zaw, and S. K. Aung, "Design and development of microcontroller based air conditioning system," *International Journal of Scientific Engineering and Technology Research*, 2014, 3(10), 2000-2004.
- [10] D. Midgley, *Centrifugal Compressor and Pump Selection*. New York: McGraw-Hill Education, 2015.
- [11] R. K. Rajput, *A Textbook of Engineering Thermodynamics*. 3rd Edition, New Delhi: Laxmi Publications Limited, 2008.
- [12] T. L. Bergman, A. S. Lavine, F. P. Incropera, and D. P. Dewitt, *Fundamentals of Heat and Mass Transfer*. 7th Edition, New York: John Wiley & Sons, 2011.
- [13] M. M. Awad, (2002). Two-Phase Flow. <http://dx.doi.org/10.5772/76201>
- [14] W. S. Susan, "Enhanced Finned-Tube Condenser Design and Optimization," A Dissertation presented in the Department of Mechanical Engineering, Georgia Institute of Technology, 2013, unpublished.

- [15] A. Cavallini, G. D. Censi, D. Col, L. Doretto, G. A. Longo, and L. Rossetto, "In-tube condensation of halogenated refrigerants," *ASHRAE Transactions*, 2002, Vol. 108, No. 1, #4507.
- [16] D. G. Rich, "The Effect of Fin Spacing on the Heat Transfer and Friction Performance of Multi-Row, Smooth Plate Fin-and-Tube Heat Exchangers," *ASHRAE Transactions*, 1973, Vol. 79, No. 2, pp. 137-145.
- [17] T. H. Lee, J. S. Lee, S. Y. Oh, M. Y. Lee, and K. S. Lee, "Comparison of Air-Side Heat Transfer Coefficients of Several Types of Evaporators of Household Freezer/Refrigerators," *International Refrigeration and Air Conditioning Conference*. 2002, Paper 611. Available: <http://docs.lib.purdue.edu/iracc/611>
- [18] M. A. Akintunde, "The Effects of Friction Factors on Capillary Tube Length," *Pacific Journal of Science and Technology*. 2007, 8(2), 238-245.
- [19] Engineers Edge. (2000). Copper Tubing HVAC Size Chart [Online]. Available: [https://www.engineersedge.com/fluid\\_flow/copper\\_tubing\\_hvac\\_size\\_chart\\_13182.htm](https://www.engineersedge.com/fluid_flow/copper_tubing_hvac_size_chart_13182.htm)
- [20] M. A. Akintunde, "Theoretical design model for vapour compression refrigeration systems," *ASME J.* 2004, 73(5), 1-14.
- [21] V. Gnielinski, "New equations for heat and mass transfer in turbulent pipe and channel flow," *Int. Chem. Engineering*, 1976, 16:359-368.



**I. F. Titiladunayo** is a Lecturer (Senior) in the Department of Mechanical Engineering at The Federal University of Technology Akure, Nigeria. He holds M.Eng. and PhD degrees in Mechanical Engineering. He has published a number of research articles in reputable engineering and professional journals. He has many years of teaching and research experience.



**R. A. Shittu** is a Teaching Assistant in the Department of Mechanical Engineering at The Federal University of Technology Akure, Nigeria. He holds M.Eng. degree in Building Services Engineering from the same University. He is a research student in the same field.